Study on Corrosion Behavior of X80 Steel under Stripping Coating by Sulfate Reducing Bacteria

Yanyu Cui
Civil Aviation University of China
Yongxiang Qin (550462668@qq.com)
Civil Aviation University of China https://orcid.org/0000-0002-6754-5844
Qingmiao Ding
Civil Aviation University of China
Yuning Gao
Civil Aviation University of China

Research article

Keywords: Sulfate reducing bacteria (SRB), Microbial corrosion, X80 steel, Electrochemistry

Posted Date: September 18th, 2020

DOI: https://doi.org/10.21203/rs.3.rs-68483/v1

Version of Record: A version of this preprint was published on January 9th, 2021. See the published version at https://doi.org/10.1186/s12896-020-00664-5.

Dear Editor,

Please find enclosed our manuscript entitled **" Study on Corrosion Behavior of X80 Steel under Stripping Coating by Sulfate Reducing Bacteria",** Rasha A. Baseer; which we would like to submit to your esteemed journal of **" Journal of Food Safety".**

The manuscript has not been previously published, is not currently submitted for review to any other journal, and will not be submitted elsewhere before a decision is made by this journal.

Thanks in advance, hoping to hear from you

Sincerely yours

Corresponding author

Yong-xiang QIN, College of Airport, Civil Aviation University of China, Tianjin, 300300, P. R. China.

Telephone +8616622980797

E-mail addresses: 550462668@qq.com

Postal Code: 300000

Study on Corrosion Behavior of X80 Steel under Stripping Coating by Sulfate Reducing Bacteria

Yan-Yu CUI[1], Yong-Xiang QIN[1], Qing-Miao DING [1], Yu-Ning GAO [1]

1College of Airport, Civil Aviation University of China, Tianjin 300300, P. R. China

[1] Correspondence: Yong-xiang QIN, College of Airport, Civil Aviation University of China, Tianjin, 300300, P. R. China. Tel: 1662298097. E-mail: 550462668@qq.com

Abstract

Background: At present, microorganism has been considered as important factors that threaten to buried pipelines with disbonded coatings. Aiming at the problem of unknown corrosion mechanism of sulfate-reducing bacteria (SRB), a series of studies have been carried out in this paper. Spectrophotometer and fluorescent labeling technology are used to study the growth and attachment of SRB in the simulated soil solution. The electrochemical behavior of X80 pipeline steel with or without SRB was researched by electrochemical methods such as open circuit potential, dynamic potential polarization curve, and electrochemical impedance spectroscopy. The microscopic morphology of the corrosion products on the surface of the sample was observed with a scanning electron microscope (SEM), and the element content of the corrosion products on the surface of the sample after corrosion was observed using X-ray energy spectrum (EDS) analysis.

Results: The results showed that the growth and reproduction of SRB caused the pH of the soil simulated solution to increase, which promoted the corrosion of X80 steel. In addition, the cathode reaction of X80 steel in a sterile environment is the reduction of H^+, and the main corrosion product is Fe oxides. When the soil simulation solution contains SRB, the cathodic reaction is controlled by both H^+ reduction and sulfide depolarization reactions, and FeS appears in the corrosion products. **Conclusion:** Although the life cycle of SRB is only about 14 days, the corrosion of X80 steel is greatly promoted by SRB, and even causes corrosion perforation, which will bring huge economic losses and serious safety hazards.

Keywords: Sulfate reducing bacteria (SRB), Microbial corrosion, X80 steel, Electrochemistry

1 Background

Microbiologically influenced corrosion (MIC) refers to microbial life activities that directly or indirectly promote the metal destruction caused by the corrosion process [1-5]. It is found in equipment in various fields such as soil, machinery, oil fields and seawater. The economic loss caused by microbial corrosion in industry is about 30-50 billion US dollars every year [6-8]. Microbial corrosion is basically bacterial corrosion, which is essentially an electrochemical corrosion [9-12]. For external corrosion of metal materials such as buried pipelines and oil storage tanks, anticorrosion layer treatment and cathodic protection are generally used. Although this slows down the corrosion rate to a certain extent, the corrosion problem still exists. As the burial time increases, the corrosion rate of buried pipelines will be further accelerated due to reasons such as anti-corrosion disbonded [13-16]. Studies have shown that sulfate-reducing bacteria, iron bacteria, iron oxidizing bacteria, and sulfur oxidizing bacteria among microorganisms have serious corrosion to metals, and SRB is considered to be one of the most important causes of microbial corrosion [17-20]. At present, National and international researchers have done a series of studies on SRB corrosion. Venzlaff et al. [21] used potential dynamics polarization measurement and found that the electrons released by the anode dissolution are directly transferred to the specific protein in the sulfate reduction site of the cell through the conductive ferrous sulfide to reduce the sulfate. This conclusion is consistent with the BCSR (Biocatalytic cathodic sulfate reduction) theory proposed by Enning [22]. Wikiel, Dong and Castaneda [23-25] believe that the solution enters the bottom of the biofilm through the porous structure of the biofilm and directly contacts the metal. Due to the anisotropy of the biofilm on the surface of the metal, the environment of the metal is different. Compared with the bacterial environment, local corrosion is more likely to occur. Brenda and Washizu [26-27] believe that biofilm has a catalytic effect, which can increase the cathode current density and accelerate the self-passivation of metal surfaces. These two conflicting theories are showing the complexity of the research on microbial corrosion mechanism.

Although national and international have done a lot of research on the corrosion of metals by SRB, due to the variety of SRB and the complex metabolism activities, there is no agreement on the corrosion mechanism of SRB at present. In addition, there are relatively few studies on SRB corrosion in special complex environments such as the peeling of buried pipeline coatings. Therefore, conducting SRB corrosion research in complex environments has practical engineering

significance and value. In this paper, the effects of SRB on the corrosion behavior of X80 steel under peeled coating were studied using various methods such as biotechnology, electrochemical experiments, morphological analysis, numerical simulation, etc., in order to provide a certain theoretical basis and data support for the safe operation of the pipeline.

2 Methods

2.1 Sample preparation

The back of the test piece was welded with copper wire, and the side and welding wire are sealed with epoxy resin. One side is used as working surface (area is 100 mm^2). A rectangular design of 10 mm×10 mm ×3 mm test specimens (X80 pipelines steel) was abraded with a series of emery paper (coarseness between 320 and 2000 mesh), subsequently washed with distilled water, ethanol and acetone and eventually dried in dry air before use. The chemical composition (mass fraction) of X80 pipeline steel is shown in Table 1.

Table 1 Chemical composition of X80 steel (wt%)

C	Si	Mn	P	S	Cr	Ni	Ti	Nb	V	Mo	Fe
0.063	0.28	1.83	0.011	0.0006	0.03	0.03	0.016	0.061	0.059	0.22	For balance

2.2 Experimental medium

The soil near the X80 pipeline in service in southwest China was put into a drying box to air-dry to remove debris, and then continued to be dried in an oven at 120°C for 10 hours to remove moisture. The dried soil and deionized water are mixed in a mass ratio of 1: 5, and the centrifugation method is used for titration test [28]. The chemical composition and content of the soil are shown in Table 2. Deionized water is used to prepare a soil simulation solution, and nitrogen is filled into the solution to exhaust the oxygen in the solution. Subsequently, an autoclave (403 K) was used about thirty minutes to kill the original microorganisms in the solution. During the experiment, keep the device well sealed to prevent oxygen from entering the solution.

Table 2 Chemical composition of soil solution

H_2O/mL	Na_2CO_3/g	NaCl/g	Na_2SO_4/g	$NaHCO_3$/g
1000	0.16	0.5125	0.1712	0.0865

2.3 Activation culture and inoculation of sulfate reducing bacteria

The Postgate Medium SRB medium (0.52 g) is weighed and placed in a sterile Erlenmeyer flask, then distilled water (100 mL) and sodium D-lactate (0.11 g) were added, stir evenly with a

sterile glass rod, adjust the culture with 5 mol/L NaOH. The prepared liquid culture medium was put into the autoclave for sterilization, and then put into the ultra-clean workbench, and cool to room temperature under the irradiation of ultraviolet light. Among them, the components of SRB medium are divided into: Yeast extract 1.0 g/L, Sodium sulfate(Na_2SO_4) 3.5 g/L、Magnesium chloride hexahydrate（$MgCl_2·6H_2O$）2.0 g/L、Ascorbic acid（$C_6H_8O_6$）0.1 g/L、Ammonium chloride（NH_4Cl）1.0 g/L、Dipotassium phosphate（K_2HPO_4）0.5 g/L、Calcium chloride（$CaCl_2$）0.05 g/L、Ferrous sulfate heptahydrate（$FeSO_4·7H_2O$）0.5 g/L、Sodium thioglycolate（$C_2H_3NaO_2S$）0.1 g/L。

The frozen purebred SRB was taken out of the refrigerator and thawed, and then the pure bacterial solution (including glycerol) in the 30 mL freezing tube was added to the prepared liquid medium (100 mL) with a pipette [29]. Put the base into a 30℃ constant temperature biochemical incubator for replacement culture, and constantly observe the liquid medium to become black, and wait for it to become completely black, indicating that the SRB cultured in intergeneration has biological activity. The experiment is divided into two groups: (a) the bacteria experimental group inoculated with SRB and (b) the sterile control group not inoculated with SRB. For the experimental group with bacteria, take 50 mL of cultivated SRB and 950 mL of simulated soil solution to mix it, and add it to the experimental device. For the sterile control group, 50 mL of deionized water was mixed with 950 mL of simulated soil solution [28].

2.4 Electrochemical experiment

The epoxy primer is sprayed on the bottom plate of the thermal spraying device to simulate the peeling of the coating. The peeling height is 1mm, the schematic diagram of the experimental test device is shown in Fig.1, and the experimental device is sterilized before the experiment. The electrochemical test was carried out on the electrochemical workstation CHI660D. The experiment used a three-electrode test system, X80 pipeline steel as the working electrode, saturated calomel electrode as the reference electrode, and the auxiliary electrode as the Pt electrode. Electrochemical experiments mainly include open circuit potential (OCP), dynamic potential polarization curve, alternating current impedance (EIS) test [6]. First, the open-circuit potential test of the working electrode is carried out, and then the dynamic potential polarization curve test is carried out after its stability. The scanning rate is 0.1 mV/s, and the scanning range is

Eocp±250 mV. The scan rate of EIS is 0.5 mV/s，The test frequency range is 10^{-2} ~ 10^{6}，The AC excitation signal is a 10 mV sine wave.

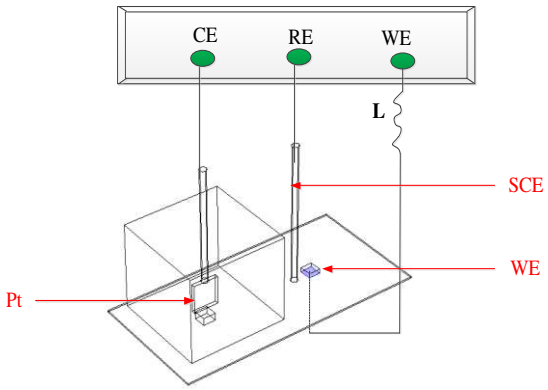

Fig.1 Schematic of experimental set-up

2.5 Soak experiment

In order to study the effect of different AC stray current density and SRB coupling on the corrosion morphology of X80 pipeline steel under peeled coating, AC current with different current density was applied to the soil solution inoculated with SRB, and the prepared electrode was placed in the experimental device Soak for 10d. The sample after soaking was fixed with 2% glutaraldehyde phosphate buffer solution for about 5 hours. After the fixation is completed, rinse with sterile saline and use alcohol of 25%, 50%, 75%, and 100% volume fraction to dehydrate about 10 minutes [29]. After the dehydration is completed, the scanning electron microscope model KYKY-EM6X00 is used to observe the microscopic morphology of the corrosion products, and the corrosion products on the surface of the sample are subjected to elemental analysis by X-ray energy spectrum analysis.

3 Result

3.1 Growth of SRB

An ultraviolet spectrophotometer was used to measure the *OD* value of the solution after X80 was immersed in the soil simulation solution for different days [30], the measurement results are shown in Fig.2. It can be seen from Fig. 2(a) that SRB is the adaptation period from the first day to the forth. This stage shows that SRB does not rapidly multiply and die after entering the new environment (soil simulation solution) from the culture medium and its number is relatively stable

overall. From the forth days to the eighth, SRB enters logarithmic growth phase, and the growth rate of SRB is the fastest in this phase. From the eighth days to the tenth, SRB enters stable growth period, and the number of SRB reaches the maximum. SRB died abruptly during the decay phase from the eighth days to the tenth, and the number decreased rapidly. From the thirteenth days to the fourteenth, SRB enters the residual stage, in which the number of SRB is relatively stable, and the total number remains at a low level. It can be seen from Fig.2 (b) that the pH of solution is relatively stable in the first 4days. The pH suddenly increased on the fifth day, and maintained a slow increase after the ninth day. This is because the number of SRB increased relatively slowly in the first 3 days, and the growth and reproduction speed of SRB accelerated from the fifth days to ninth. This process continued to consume H^+, which in turn caused the solution pH to increase continuously. After entering the stable growth phase and decay period, SRB multiplies very slowly, so the pH value of the solution is relatively stable.

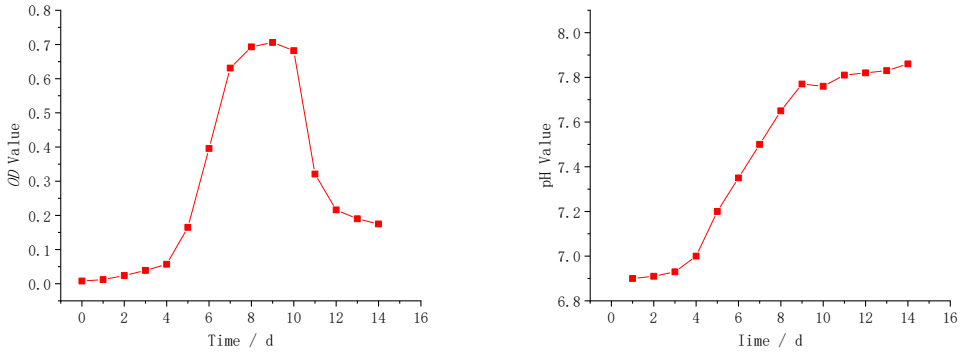

Fig.2 Variations of *OD* value (a) and pH value (b) with time

In addition, acridine orange (AO) was used to fluorescently label the SRB on the sample surface. Because acridine orange has good membrane permeability, it can specifically bind to nucleic acid substances in cells after contact with bacteria, and the biologically active SRB produced by the excitation lamp is green, and the inactive SRB is red, green and red mixed together appear yellow. At the same time, Imagepro Plus software was used to count the number of SRB attached to the sample surface and the results are shown in Fig.3 [28]. It can be seen from Fig. 3 that the amount of SRB attached to the surface of the sample increases with the increase of the soaking time. At the third day, the amount of SRB attached to the surface of the sample was small and partially inactivated; at the sixth day, the amount of SRB adhered to the surface of the sample increased, and the number in the inactivated state decreased. At the ninth day, the amount of SRB adhesion

on the surface of the sample significantly increased. On the twelfth day, the amount of SRB adhesion on the surface of the sample continued to increase, but most of them are in an inactive state.

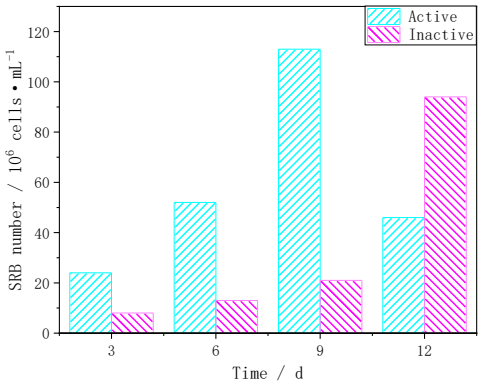

Fig.3 The number of SRB on the surface changes with the immersion time

3.2 Effect of SRB on the electrochemical behavior of X80 steel

The open circuit potential (E_{OCP}) of X80 pipeline steel in bacteria and sterile soil simulation solution changes with time as shown in Fig.4. It can be seen from Fig.4 that the open circuit potential of X80 steel in the soil simulation containing SRB changes with time in accordance with the change rule in the sterile solution. With the increase of the immersion time, the open circuit potential exhibits a change rule of first negative shift and then positive shift [12].

This is because in the early stage of immersion, the surface of the sample is relatively smooth, and its tendency to corrode increases with time. After six days of immersion, the corrosion products on the surface of the sample gradually increased and accumulated on the surface to form a corrosion product film, which hindered the corrosion of the substrate by harmful ions in the solution, resulting in a reduction in the corrosion tendency. In addition, the open circuit potential in the sterile solution is entirely in the SRB environment, so X80 steel has a greater tendency to corrode in the simulated soil solution with SRB.

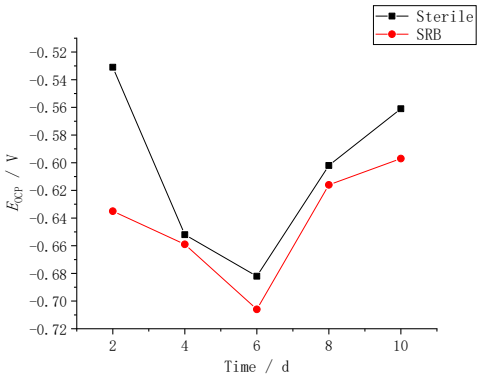

Fig.4 Open circuit potential of X80 steel in bacteria and sterile environment

The polarization curve test was performed on X80 steel soaked in sterile soil simulation solution and SRB-containing soil simulation solution for 5 days and 10 days. The results are shown in Fig.5. It can be seen from Fig.5 that in the soil simulation solution containing SRB, the polarization curve of X80 steel is located at the upper left in a sterile environment, indicating that X80 steel has a greater tendency to corrode in a bacteria environment. Fitting and analyzing the polarization curve to obtain its corresponding electrochemical parameters, as shown in Table 3. It can be seen from Fig.5 and Table 3 that when the immersion time is the same, the corrosion current density of X80 steel in the soil simulation solution containing SRB is about 7 times that of the sterile environment, indicating that SRB greatly promotes the corrosion of X80 steel in the soil. The corrosion rate of X80 steel on the 5th day is less than that on the 10th day, and the rule of bacteria and aseptic environment is consistent. This conclusion is consistent with the change of the open circuit potential.

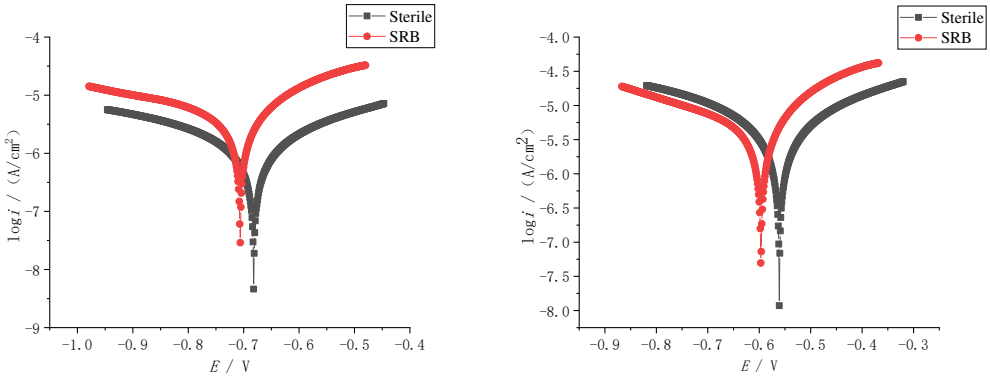

（a）5d **（b）10d**

Fig.5 Potential polarization curve of X80 steel in sterile and bacteria soil simulation solution

Table 3 Fitting results of polarization curves in sterile and bacteria soil simulated solutions

Environment	Time (d)	E_{corr} (V)	i_{corr} (μA/cm^2)	β_a (mV·dec^{-1})	β_c (mV·dec^{-1})

Sterile	5	-0.682	1.064	727.0	651.4
	10	-0.602	1.535	711.9	669.4
SRB	5	-0.647	7.922	735.4	659.1
	10	-0.552	10.95	719.5	663.1

In order to further research the effect of SRB on the corrosion behavior of X80 steel in the soil simulation solution, the AC impedance of X80 steel immersed in the sterile and bacteria soil simulation solution at different times was measured. The results are shown in Fig. 6, where Z' represents the real part of the AC impedance spectrum, and Z'' represents the imaginary part of the AC impedance spectrum [31]. It can be seen from Fig. 6(a) that the resistance arc and capacitance radius of X80 steel in the sterile soil simulation solution increase with the increase of the sample soaking time, and then gradually decrease after a slight increase. This is because the corrosion products continue to increase with the extension of time in 0~4d, and the diffusion rate of corrosion products is much smaller than the generation rate, resulting in the accumulation of corrosion product film on the surface of X80 steel, so the corrosion rate of the substrate is reduced. On the 4th to 10th days, the diffusion rate of corrosion products increases and the generation rate decreases. The corrosion product film on the surface of the sample begins to crack or even fall off, causing harmful ions in the solution to contact the remaining X80 substrate through the gap, forming crevice corrosion and accelerating the corrosion rate of the substrate. On the other hand, the $Fe(OH)_2$ formed by the combination of Fe^{2+} and OH^- in the solution forms a corrosion couple with the X80 matrix, which further accelerates the corrosion rate. With the continuous increase of SRB in 4~8d, the impedance arc and capacitive reactance radius gradually decrease. This is because SRB consumes H^+ on the surface of X80 steel, resulting in an increase in the corrosion rate of the sample [32]. The chemical reaction on the surface of X80 steel continued to prolong with the immersion time (10th day). SRB formed a dense biofilm on the surface of X80 steel, which caused the corrosion rate of the substrate to decrease and the corresponding impedance arc radius to increase. At the same time, the sulfide produced by SRB during growth and metabolism attaches to the gap of the biofilm, which further strengthens the effect of the biofilm on the surface of X80 steel on the diffusion of solution ions [33]. According to Fig. 6, it can be seen that the impedance radius of the bacteria environment at the same immersion time is significantly smaller

than that in the sterile environment, indicating that X80 steel is more prone to corrosion in the soil simulation solution containing SRB.

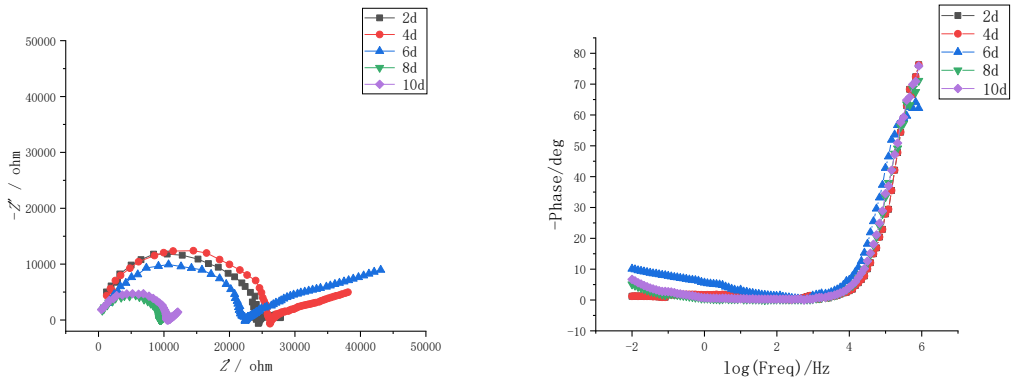

（a）Aseptic environment

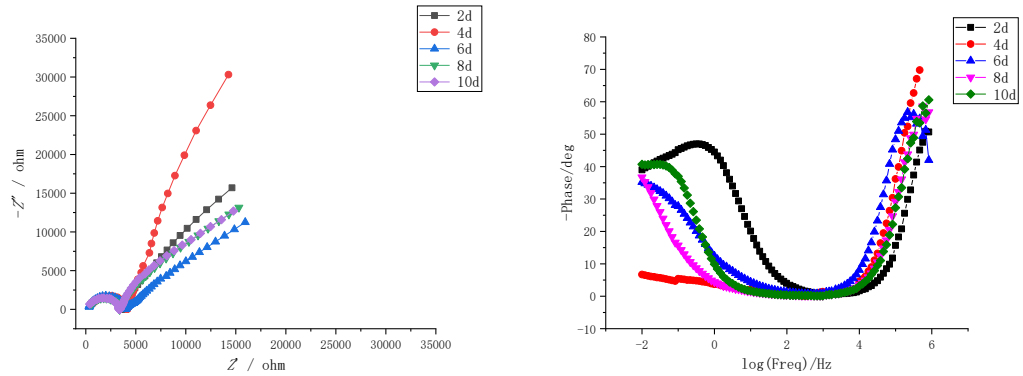

（b）Bacterial environment

Fig.6 Nyquist diagram and Bode diagram of X80 steel in a sterile and bacteria-free environment

In order to clear analyze the impedance data, the software of ZSimWin was used to fit the impedance spectrum. The equivalent circuit can be fitted with a model of two time constants. The equivalent circuit is shown in Fig.7, and the fitting result is shown in Fig.8. Where R_s is the resistance of the simulated soil solution, R_b and R_f represent the resistance of the corrosion products, R_{ct} represents the charge transfer resistance, Q_{dl} represents the electric double layer capacitance, Q_b and Q_f represent different meanings, in the sterile soil simulation solution, Q_b represents the corrosion product film Formed capacitive reactance. In the SRB-containing soil simulation solution, the microbial film represented by Q_f and the corrosion product film form a capacitive reactance under the combined action. The state variables considered in this experiment include the effects of electrode potential and corrosion product layer or biofilm, so it is the

polarization resistance $R_p=(Z_F)_{w=0}=R_f+R_{ct}$ that reflects the change in the corrosion rate of X80 steel in the experimental system [34]. In the formula, Z_F is the Faraday impedance of the experimental system, which is equivalent to the impedance of the experimental system after removing the soil simulated solution resistance R_s and the illegal Faraday impedance Z_{NF}.

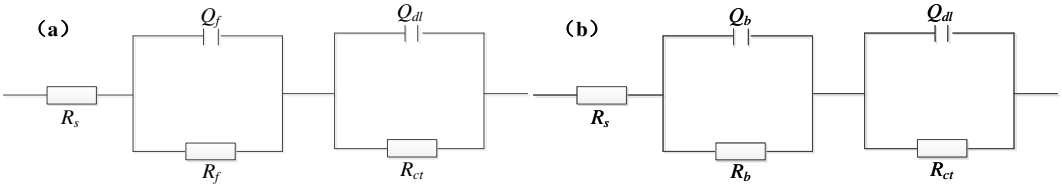

Fig. 7 The equivalent circuits of X80 steel in (a) the sterile and (b) SRB inoculated

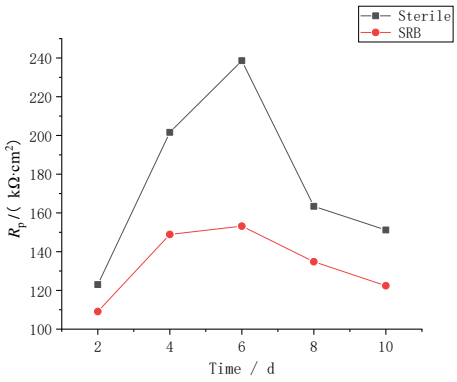

Fig. 8 Polarization resistance changes with time

It can be seen from Fig. 8 that the polarization resistance R_p of X80 steel in the aseptic and SRB-containing soil simulation solutions showed a variation rule that increased first and then decreased with the increase of the soaking time, and reached the maximum value on the sixth day. This is because the formation rate of corrosion products on the sample surface is much greater than the immersion diffusion rate, which results in the accumulation of corrosion on the surface of the sample gradually to form a corrosion product film, and the density of the corrosion product film gradually increases. With the further increase of the immersion time, the spread rate of the corrosion products on the surface of the sample is greater than the generation rate, and defects such as cracks appear on the corrosion product film, which in turn leads to a decrease in polarization resistance. In addition, under the action of SRB, the diffusion rate of corrosion products on the surface of the sample is accelerated, so the polarization resistance of the sample in the SRB environment is less than that in the sterile environment. This shows that SRB promotes the corrosion of X80 steel, and this conclusion is consistent with the analysis results of open circuit potential and polarization curve.

3.3 Corrosion product morphology and product analysis

The corrosion product morphology of X80 steel after being immersed in sterile and SRB-containing soil simulation solution for 10 days is shown in Fig.9. EDS analysis was performed on the surface of the corrosion products on the surface of the sample shown in Fig. 9, which the results are shown in Fig.10.

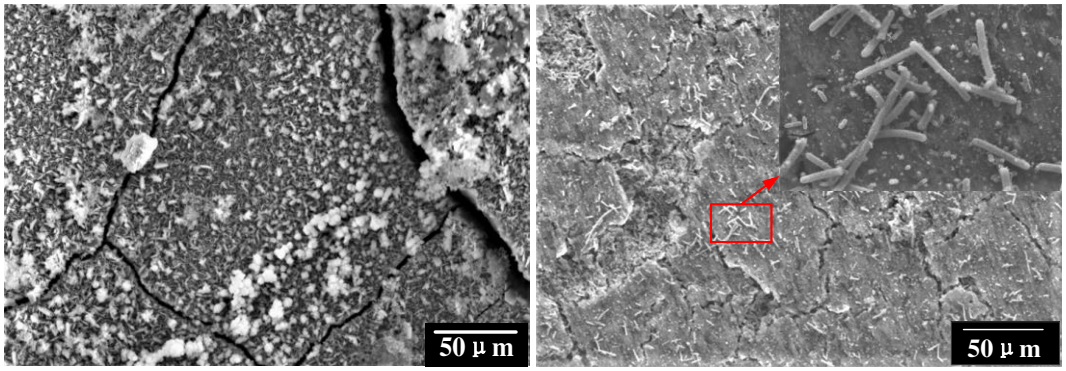

（a）Aseptic environment （b）Bacterial environment

Fig. 9 Micro-morphology of corrosion products on the sample surface

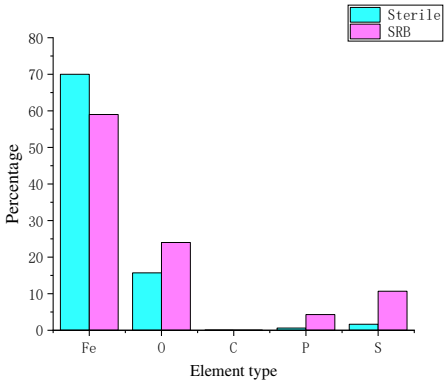

Fig. 10 EDS analysis results of corrosion products

It can be seen from Fig. 9 that after immersing X80 steel in sterile simulated soil solution for 10 days, the surface corrosion products are flocculent relative to the fluffy products, and the corrosion product film cracks. In the presence of bacteria, a large amount of SRB can be clearly observed on the surface of the sample, and a dense corrosion product film is formed on the surface. As can be seen from Fig. 10, when SRB is present in the simulated soil solution, the proportion of Fe on the surface of the sample decreases, and the proportion of O, P, and S increases significantly [35]. This is because the corrosion products of X80 steel in a sterile environment are mainly Fe oxides. When SRB is present in the environment, the metabolic activity of SRB on the sample surface participates in the corrosion process, and FeS is generated on the sample surface [7].

Therefore, the cathodic process of corrosion of X80 steel in SRB-containing soil is the depolarization reaction of phosphide and SO_4^{2-}, and the anode is the dissolution of Fe, which further verifies that SRB promotes the corrosion of X80 steel [36]. The corrosion mechanism is shown in equations (1) to (6), and the specific reaction path is shown in Fig.11 [3].

Anode reaction $4Fe \rightarrow 4Fe^{2+}+8e^{-}$ （1）

Ionization of water $8H_2O \leftrightarrow 8H^{+}+8OH^{-}$ （2）

Cathodic reaction $8H^{+}+8e^{-} \rightarrow 8H$ （3）

Cathode reaction with bacteria $SO_4^{2-}+8H \xrightarrow{SRB} S^{2-}+4H_2O$ （4）

Primary corrosion products $Fe^{2+}+S^{2-} \rightarrow FeS$ （5）

Secondary corrosion products $3Fe^{2+}+6OH^{-} \rightarrow 3Fe(OH)_2$ （6）

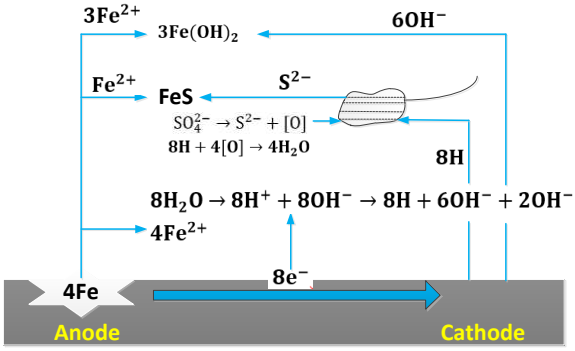

Fig. 11 SRB corrosion diagram

3.4 Numerical Simulation

The "secondary current distribution and dilute matter transfer" interface were used to simulation and the three-dimensional physical model was established as shown in Fig.12. Arbitrarily take a microcell from the stable, passive corrosion model shown in Fig.12, set its side length to d_x, d_y, d_z, where the volume $d_v = d_x d_y d_z \neq 0$, and the microcell structure is shown in Fig.13. .

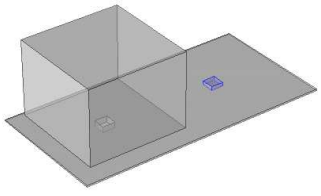

Fig.12 Physical model

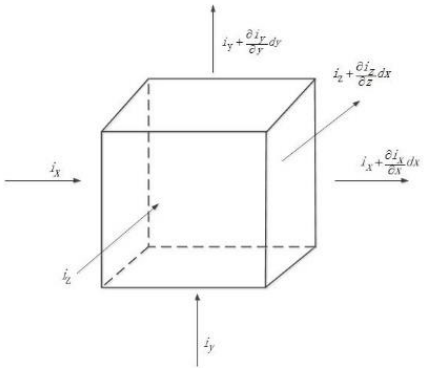

Fig. 13 Schematic diagram of micro-body current flow

Suppose that the current flowing into the cell in the *x* direction and the current flowing out in the model are equal, namely:

$$i_x dydz = (i_x + \frac{\partial i_x}{\partial x} dx)dydz \qquad (7)$$

Similarly, in the *y* direction:

$$i_y dxdz = (i_y + \frac{\partial i_y}{\partial y} dy)dxdz \qquad (8)$$

in the *z* direction:

$$i_z dxdy = (i_z + \frac{\partial i_z}{\partial z} dz)dxdy \qquad (9)$$

From the above equations (7), (8), (9) we can get:

$$-\frac{1}{\rho}\nabla^2\varphi = 0 \qquad (10)$$

That is to say, the Laplace equation is used as the control equation of the potential distribution in the corrosion field. The surface corrosion rate of X80 steel after immersion in simulated soil solution for 10 days, as shown in Fig.14. It can be found from Fig.14 that the maximum corrosion rate of the bacteria environment is about 3.5 times that of the sterile environment.

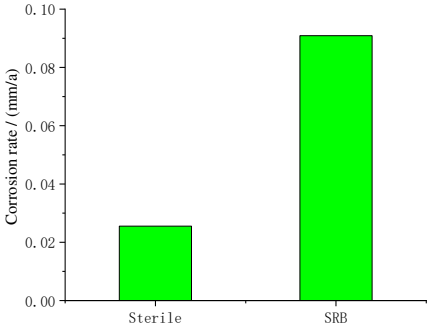

Fig. 14 Corrosion rate of X80 steel

4 Conclusions

(1) During the growth and reproduction of SRB, SO_4^{2-} is reduced and the H+ in the simulated soil solution is consumed, resulting in an increase in the pH of the solution. The change of open circuit potential of X80 steel with time in sterile and bacteria environment is basically the same, and the corrosion tendency in SRB-containing simulated soil solution is greater.

(2) Electrochemical experiments show that SRB promotes the corrosion of X80 steel in the simulated soil solution. The COMSOL simulation results show that the maximum corrosion rate of the bacteria environment is about 3.5 times that of the sterile environment.

(3) The corrosion products of X80 steel in sterile soil simulation solutions are mainly Fe oxides. When the soil simulation solution contains SRB, the content of P and S elements in the corrosion products of X80 steel increases sharply, indicating that the cathode reaction is the depolarization reaction of phosphide and sulfide, and the anode is the dissolution of Fe.

Abbrevitions

SRB: Sulfate-reducing bacteria; SEM: Scanning electron microscope; EDS: X-ray energy spectrum; MIC: Microbiologically influenced corrosion; BCSR: Biocatalytic cathodic sulfate reduction.

Ethics approval and consent to participate

This research does not involve any ethical issues.

Consent for publication

Not applicable.

Availability of data and materials

All data, raw and processed, is readily available from the corresponding author on request.

Competing Interests

“The authors declare that there is no conflict of interests regarding the publication of this article.”

Funding

(1) 2019 Tianjin Graduate Student Research and Innovation Project: Forecasting the service life of the apron pipe network under the coupling of multiple corrosion factors (2019YJSS069)

(2) The basic scientific research service fee of the Central University of Civil Aviation University of China (3122019107-Research on the influence mechanism of microbes on the failure of aircraft overall fuel tank coating-aluminum alloy system) and Civil Aviation Safety Capacity Building Fund (Construction of safety evaluation system for multibranch complex annular apron pipe network).

Authors' contribution

Conceptualization, QMD; Methodology, YXQ; Software, YXQ and YNG; Validation, YYC, YXQ; Formal analysis, YXQ and YNG; Investigation, QMD; Resources, QMD; Data curation, QMD and YXQ; Writing—original draft preparation, YXQ; Writing—review and editing, YYC, YXQ, QMD, YNG; Funding acquisition, YXQ and YYC. All authors consent and approved the final version of the manuscript.

Acknowledgements

We would like to thank Dr. Xiaoning Shen for his assistance in the simulation techniques. We also would like to gratefully thank and acknowledge Miss. Bo Shi for the precise storage of SRB.

References

1. Xie F, Li X, Gao S F, Wang D, Wu M (2018) Research progress on stress corrosion cracking behavior of X80 pipeline steel in soil environment containing sulfate-reducing bacteria. Materials Guide 31(13): 69-77.
2. Chen X, Li S B, Zheng Z S, Xiao J B, Ming N X (2020) He Chuan. Research on microbial corrosion behavior of X70 pipeline steel in Daqing soil environment. Journal of Chinese Society for Corrosion and protection 40(02):175-181.
3. Xu P, Ren H Y, Wang C Z, Zhang Y J (2019) Research progress of mixed microbial corrosion and analysis methods on metal surfaces. Surface Technology 48(01): 216-224.
4. Li X, Sun C (2018) Synergistic Effect of Carbamide and Sulfate Reducing Bacteria on

Corrosion Behavior of Carbon Steel in Soil. International journal of corrosion 2018:7491501.1-7491501.14.

5. Ubong E, Omar F, Jerzy S (2018) Effect of benzothiazole biocide on SRB-induced biocorrosion of hot-dip galvanized steel. Engineering Failure Analysis 93:111-121.
6. Sun F Y, Yang X, Lu Y, Shang K (2018) Effects of SRB on microbial corrosion behavior of X100 pipeline steel in saline soil. Pipeline Technology and Equipment, (05): 42-46.
7. Deyab M A. Efficiency of cationic surfactant as microbial corrosion inhibitor for carbon steel in oilfield saline water[J]. Journal of Molecular Liquids, 2018, 255(1):550-555.
8. Sun F Y, Zhao G X, Yang D P (2014) Microbial corrosion characteristics of X100 pipeline steel in Korla soil simulation solution. Materials Guide 28(24): 47-51.
9. Zhang W Y (2017) Advances in marine microbial corrosion research. Comprehensive Corrosion Control 31(01): 8-12.
10. Vaithiyanathan S, Chandrasekaran K, Barik R C (2018) Green biocide for mitigating sulfate-reducing bacteria influenced microbial corrosion. Biotech 8(12):495.
11. Chilkoor G, Karanam S P, Star S (2018) Hexagonal Boron Nitride: The Thinnest Insulating Barrier to Microbial Corrosion. Acs Nano 12(3):2242-2252.
12. Wu M, Guo Z W, Xie F, Wang D, Wang Y C (2018) Research progress on corrosion behavior of pipeline steel under the action of anions and sulfate-reducing bacteria. Materials Guide 32(19): 3435-3443.
13. Cui Y, Qin Y, Dilimulati D (2019) The Effect of Chlorine Ion on Metal Corrosion Behavior under the Scratch Defect of Coating. International Journal of Corrosion 1-11.
14. Xu P, Ren H Y, Wang C Z (2019) Research progress of mixed microbial corrosion and analysis methods on metal surfaces. Surface Technology 48(1).
15. Deng P C, Liu Q B, Li Z Y (2018) Research on the corrosion behavior of X70 pipeline steel in tropical seawater-sea mud transition zone. Journal of Chinese Society for Corrosion and protection 38(05):9-17.
16. Jing Q, Liu L, Xie J F, Wang P (2018) Effect of sulfate reducing bacteria on corrosion behavior of Q235 steel in corrosion scale samples of oil pipelines. Corrosion and Protection, 39(01): 6-10+ 16.

17. Venzlaff H, Stratmann M, Mayrhofer K (2013) Accelerated cathodic reaction in microbial corrosion of iron due to direct electron uptake by sulfate-reducing bacteria. Corrosion Science 66(1):88-96.
18. Sheng X, Ting Y P, Pehkonen S O (2007) The influence of sulphate-reducing bacteria biofilm on the corrosion of stainless steel AISI 316. Corrosion Science 49(5):0-2176.
19. Devatha C P, Jagadeesh K, Patil M (2018) Effect of Green synthesized iron nanoparticles by Azardirachta Indica in different proportions on antibacterial activity. Environmental Nanotechnology Monitoring & Management 9:85-94.
20. Wikieł A J, Datsenko I, Vera M (2014) Impact of desulfovibrio alaskensis biofilms on corrosion behaviour of carbon steel in marine environment. Bioelectrochemistry 97(1):52-60.
21. Venzlaff H, Stratmann M , Mayrhofer K (2013) Accelerated cathodic reaction in microbial corrosion of iron due to direct electron uptake by sulfate-reducing bacteria[J]. Corrosion Science 66(1):88-96.
22. Enning D, Venzlaff H, Garrelfs J (2012) Marine sulfate-reducing bacteria cause serious corrosion of iron under electroconductive biogenic mineral crust[J]. Environmental Microbiology 14(7):1772-1787.
23. Wikieł AJ, Datsenko I, Vera M (2014) Impact of desulfovibrio alaskensis biofilms on corrosion behaviour of carbon steel in marine environment. Bioelectrochemistry 97(1):52-60.
24. Dong Z H, Shi W, Ruan H M (2011) Heterogeneous corrosion of mild steel under SRB-biofilm characterised by electrochemical mapping technique. Corrosion Science 53(9):0-2987.
25. Castaneda H, Benetton X D (2008) SRB-biofilm influence in active corrosion sites formed at the steel-electrolyte interface when exposed to artificial seawater conditions. Corrosion Science 50(4):0-1183.
26. Little B J, Lee J S, Ray R I (2008) The influence of marine biofilms on corrosion: A concise review. Electrochimica Acta 54(1):2-7.
27. Washizu N, Katada Y, Kodama T (2004) Role of H2O2 in microbially influenced ennoblement of open circuit potentials for type 316L stainless steel in seawater. Corrosion Science 46(5):0-1300.

28. Qing Y , Bai Y , Xu J (2019) Effect of Alternating Current and Sulfate-Reducing Bacteria on Corrosion of X80 Pipeline Steel in Soil-Extract Solution. Materials 12(1).
29. Alabbas F M , Williamson C , Bhola S M (2013) Influence of sulfate reducing bacterial biofilm on corrosion behavior of low-alloy, high-strength steel (API-5L X80). International Biodeterioration & Biodegradation 78:34-42.
30. Antony P J, Raman R K S, Mohanram R (2008) Influence of thermal aging on sulfate-reducing bacteria (SRB)-influenced corrosion behaviour of 2205 duplex stainless steel. Corrosion ence 50(7):1858-1864.
31. Jie Z, Xiaolong L I, Jiangwei W (2018) Influence of calcareous deposit on corrosion behavior of Q235 carbon steel with sulfate-reducing bacteria. Journal of Ocean University of China 16(006):1213-1219.
32. Liu Q, Li Z, Liu Z Y (2017) Effects of H2S/HS on Stress Corrosion Cracking Behavior of X100 Pipeline Steel Under Simulated Sulfate-Reducing Bacteria Metabolite Conditions. Journal of Materials Engineering and Performance 26(3):2763-2775.
33. Zhao Y, Fu Z, Chen X (2018) Bioremediation process and bioremoval mechanism of heavy metal ions in acidic mine drainage. Chemical Research in Chinese Universitie 34(1):1-6.
34. Yousuf I, Arjmand F, Tabassum S (2019) Design and synthesis of a DNA intercalative half-sandwich organ ruthenium (ii)–chromone complex: cytotoxicity evaluation and topoisomerase Iα inhibition assay. New Journal of Chemistry 43(14):5475-5487.
35. Jia R, Wang D, Jin P (2019) Effects of ferrous ion concentration on microbiologically influenced corrosion of carbon steel by sulfate reducing bacterium Desulfovibrio vulgaris. Corrosion ence 153(JUN.):127-137.
36. Wei W, Jiang Y U, Wang Y (2018) Effect of SRB-zeolite technology on immobilization of lead in soil. Shenzhen Daxue Xuebao (Ligong Ban)/Journal of Shenzhen University ence and Engineering 35(6):597.

Figures

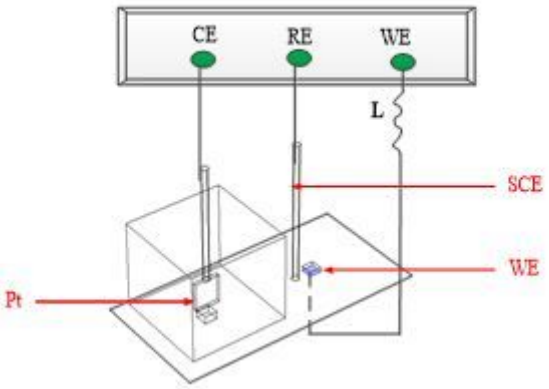

Figure 1

Schematic of experimental set-up

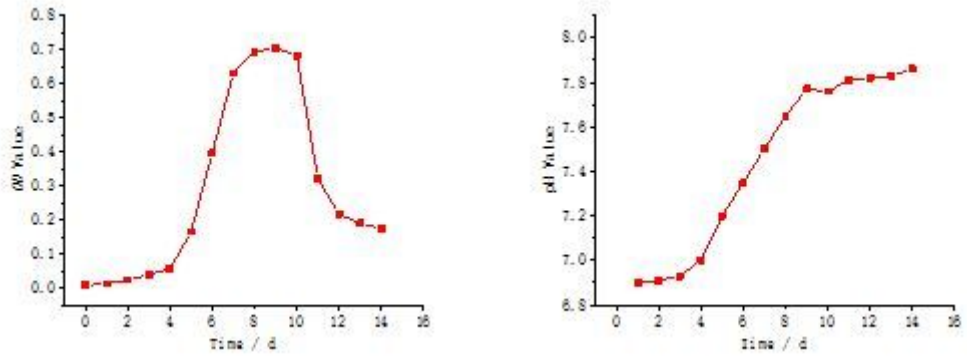

Figure 2

Variations of OD value (a) and pH value (b) with time

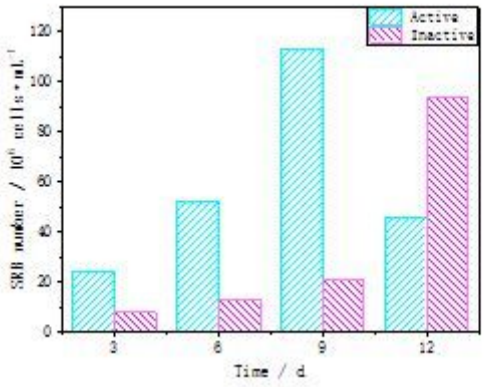

Figure 3

The number of SRB on the surface changes with the immersion time

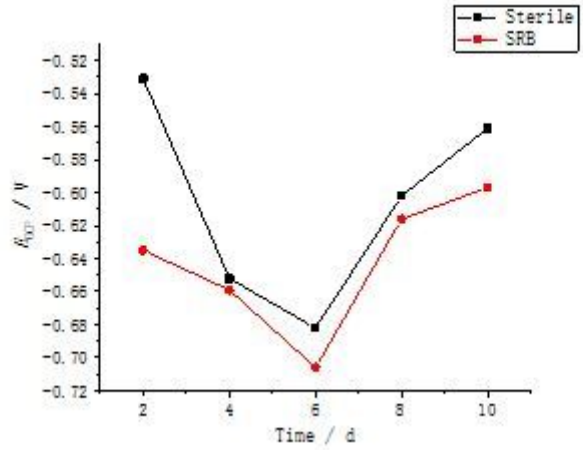

Figure 4

Open circuit potential of X80 steel in bacteria and sterile environment

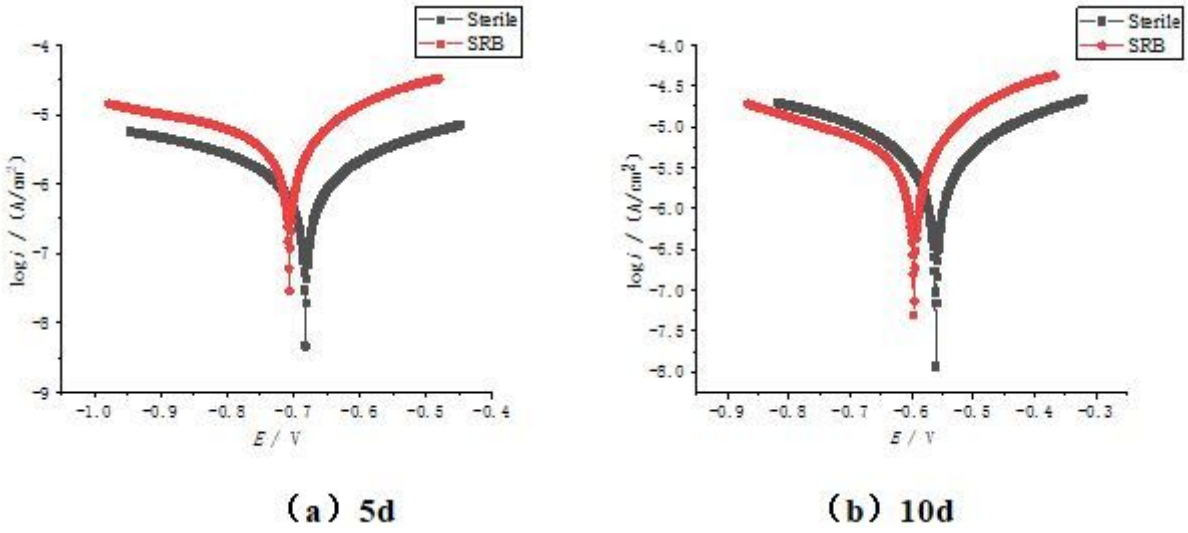

（a）5d （b）10d

Figure 5

Potential polarization curve of X80 steel in sterile and bacteria soil simulation solution

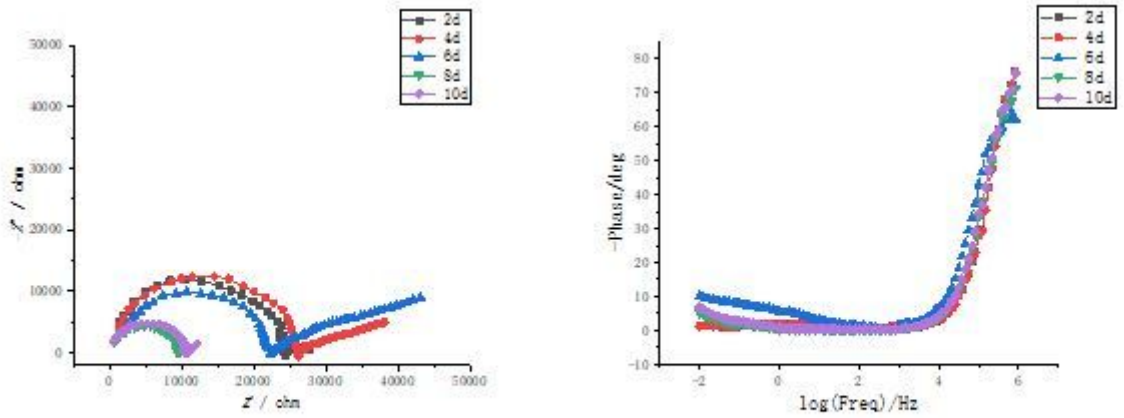

（a）Aseptic environment

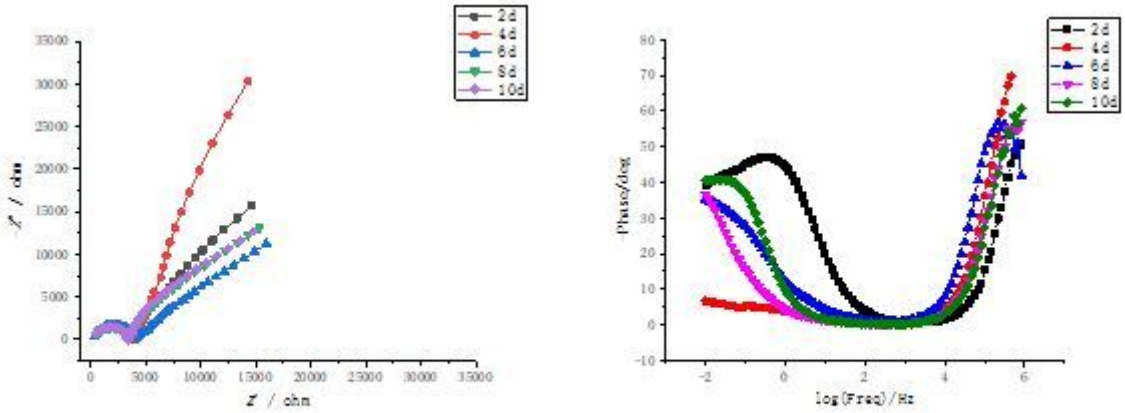

（b）Bacterial environment

Figure 6

Nyquist diagram and Bode diagram of X80 steel in a sterile and bacteria-free environment

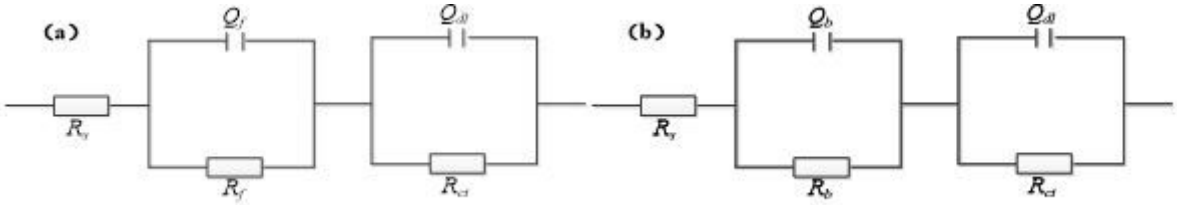

Figure 7

The equivalent circuits of X80 steel in (a) the sterile and (b) SRB inoculated

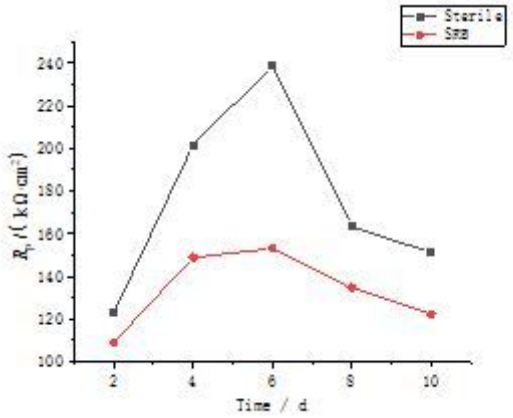

Figure 8

Polarization resistance changes with time

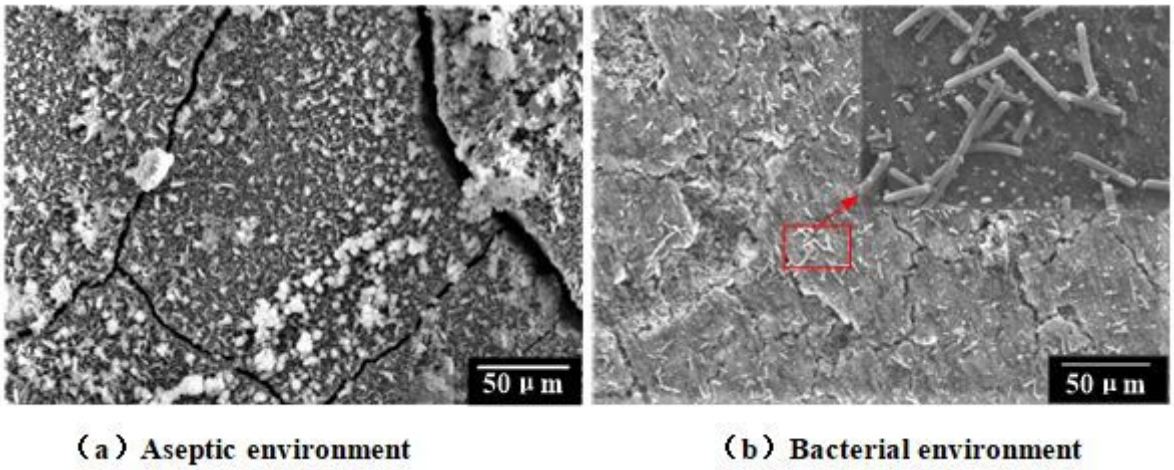

（a）Aseptic environment （b）Bacterial environment

Figure 9

Micro-morphology of corrosion products on the sample surface

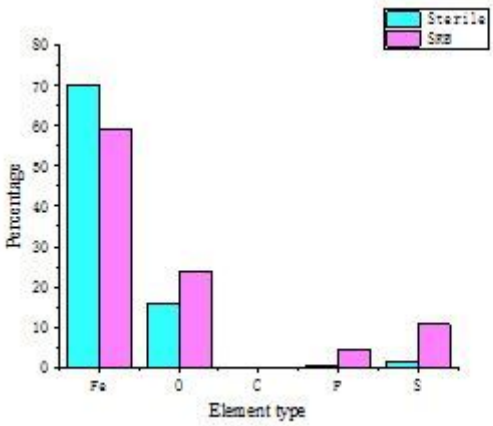

Figure 10

EDS analysis results of corrosion products

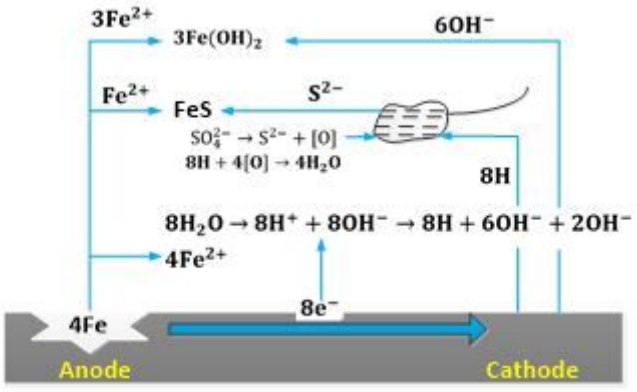

Figure 11

SRB corrosion diagram

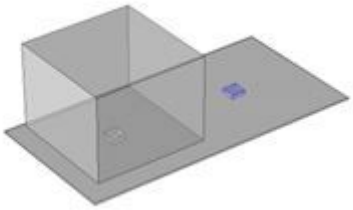

Figure 12

Physical model

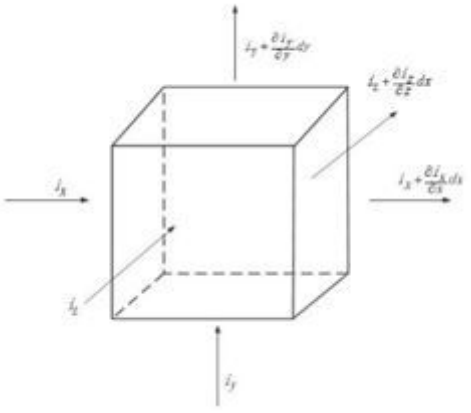

Figure 13

Schematic diagram of micro-body current flow

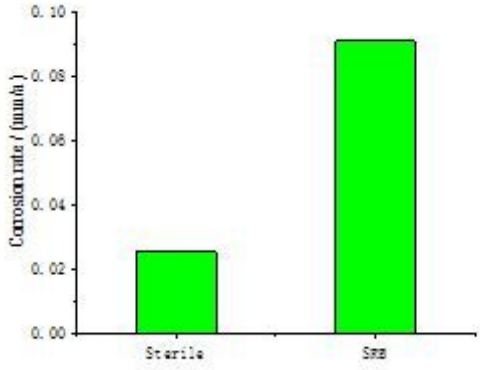

Figure 14

Corrosion rate of X80 steel